Inter-Protein Coupling Enhances the Electrocatalytic Efficiency of Tobacco Peroxidase Immobilized at a Graphite Electrode

ARTICLE *in* ANALYTICAL CHEMISTRY · OCTOBER 2015

Impact Factor: 5.64 · DOI: 10.1021/acs.analchem.5b01710

analytical chemistry

Article

pubs.acs.org/ac

Interprotein Coupling Enhances the Electrocatalytic Efficiency of Tobacco Peroxidase Immobilized at a Graphite Electrode

José Luis Olloqui-Sariego,[†] Galina S. Zakharova,[‡] Andrey A. Poloznikov,[§] Juan José Calvente,[†] Dmitry M. Hushpulian,[§] Lo Gorton,[∥] and Rafael Andreu*[,†]

[†]Department of Physical Chemistry, University of Sevilla, Profesor García González 1, 41012, Sevilla, Spain

[‡]A.N. Bach Institute of Biochemistry, Russian Academy of Sciences, Leninsky Prospect 33/2, Moscow, 119071, Russia

[§]Department of Chemistry, Lomonosov Moscow State University, Vorob'evy Gory 1, Moscow, 119991, Russia

[∥]Department of Biochemistry and Structural Biology, University of Lund, Kemicentrum, Box 118, 221 00, Lund, Sweden

Supporting Information

ABSTRACT: Covalent immobilization of enzymes at electrodes via amide bond formation is usually carried out by a two-step protocol, in which surface carboxylic groups are first activated with the corresponding cross-coupling reagents and then reacted with protein amine groups. Herein, it is shown that a modification of the above protocol, involving the simultaneous incubation of tobacco peroxidase and the pyrolytic graphite electrode with the cross-coupling reagents produces higher and more stable electrocatalytic currents than those obtained with either physically adsorbed enzymes or covalently immobilized enzymes according to the usual immobilization protocol. The remarkably improved electrocatalytic properties of the present peroxidase biosensor that operates in the 0.3 V ≤ E ≤ 0.8 V (vs SHE) potential range can be attributed to both an efficient electronic coupling between tobacco peroxidase and graphite and to the formation of intra- and intermolecular amide bonds that stabilize the protein structure and improve the percentage of anchoring groups that provide an adequate orientation for electron exchange with the electrode. The optimized tobacco peroxidase sensor exhibits a working concentration range of 10−900 μM, a sensitivity of 0.08 A M^{-1} cm^{-2} (RSD 0.05), a detection limit of 2 μM (RSD 0.09), and a good long-term stability, as long as it operates at low temperature. These parameter values are among the best reported so far for a peroxidase biosensor operating under simple direct electron transfer conditions.

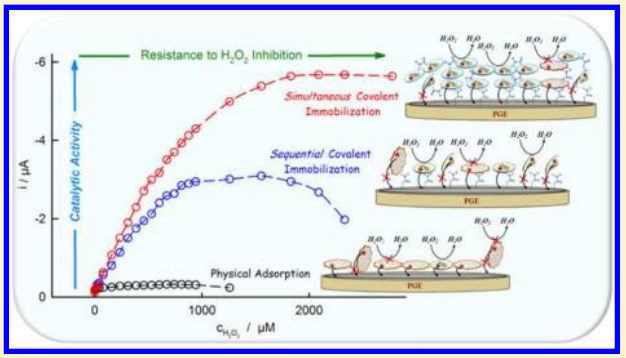

Immobilization of enzymes onto electrode surfaces has attracted considerable attention due to its potential applications in a variety of fields, such as electrocatalysis, biosensors, bioelectronics, biofuel cells, and green chemistry.[1−4] Construction of devices based on direct electron exchange between proteins and electrodes offers advantages from the point of view of selectivity and design, but it has to circumvent the problem posed by the low electronic conductivity of the polypeptide matrix that makes electron transfer between proteins and electrodes prohibitively slow for most orientations of the immobilized protein. In spite of these difficulties, direct electron transfer between several electrode surfaces and more than 40 redox enzymes has been observed already, paving the way for the development of "third generation" biosensors.

Plant peroxidases, and particularly horseradish peroxidase (HRP), have been used extensively in bioanalytical chemistry to quantify hydrogen peroxide content and as labels in electrochemical DNA and immunosensor assays.[2,5] The accepted catalytic cycle of horseradish peroxidase in a direct electron transfer configuration proceeds through the oxidation of the native ferric form of the enzyme by hydrogen peroxide to form Compound I. Then, Compound I accepts one electron from the electrode to form Compound II, which is subsequently reduced to the initial ferric form by accepting a second electron from the electrode.[6] This mechanism is expected to apply also for anionic tobacco peroxidase (TOP), which was early recognized as a promising building block for biosensors due to its high stability and substrate specificity.[7−9] A variety of strategies for immobilization of tobacco peroxidase have been reported, including physisorption on solid substrates, such as bare gold[10] and graphite[11−14] and on self-assembled thiol monolayers[15] or, alternatively, it has been embedded into a redox-active polymer gel.[16]

In this work we show how the simultaneous incubation and deposition of a mixture of TOP and the crossing coupling agents 1-ethyl-3-(3-(dimethylamino)propyl) carbodiimide (EDC) and *N*-hydroxysulfosuccinimide (NHS), which is likely to produce an extensive intra- and interprotein coupling, results

Received: May 6, 2015
Accepted: October 6, 2015

DOI: 10.1021/acs.analchem.5b01710
Anal. Chem. XXXX, XXX, XXX−XXX

in a significant enhancement of the electrocatalytic hydrogen peroxide reduction and an overall improvement of the biosensor performance. This protocol differs from the usual immobilization procedure, which involves an initial surface activation with the coupling agents, followed by extensive washing and enzyme incubation.[17] Uncontrolled physisorption of enzymes on the covalently immobilized monolayer often takes place during this incubation step. This excess of enzymes is usually considered to be detrimental for the biosensor performance, since it may hamper the substrate access to the innermost enzymatic layer and may induce a conformational distortion leading to enzyme inactivation.[18] In stark contrast with these assumptions, we have observed a significant improvement in both catalytic current and stability when enzymes and coupling agents are mixed in the incubation solution, leading presumably to a cross-linked multilayered catalytic film.[19−21] Cross-linking of *r*-TOP in solution is shown to yield exclusively dimers, whose immobilization on graphite produces electrocatalytic currents similar to those obtained with our simple one-step immobilization protocol. The improved catalytic characteristics of our biosensor can be attributed to a larger amount of properly oriented enzymes and to the formation of a favorable environment that preserves the biocatalytic activity in the presence of high hydrogen peroxide concentrations (up to 2 mM at 0 °C). The significance of these results is reinforced by a comparison with the electrocatalytic response recorded when the enzyme was either physically adsorbed or immobilized on the graphite surface by the common covalent immobilization technique.

MATERIALS AND METHODS

Enzyme Production. Wild-type recombinant TOP (*r*-TOP, hydrogen peroxide oxidoreductase, EC 1.11.1.7) was expressed in the form of inclusion bodies in *E. coli* BL21(DE3)CodonPlus cells as was described earlier.[22] The construction of the expression vector and the procedure of *r*-TOP expression, refolding, and purification are covered in detail elsewhere.[22] Briefly, biomass from 600 mL of culture medium was disrupted and the precipitate of inclusion bodies was washed, solubilized in 6 M urea, and added drop by drop to the refolding medium, containing 1.8 M urea, 0.1 mM DTT, 0.5 mM oxidized glutathione, 3 mM $CaCl_2$, 5 μM hemin, 5% glycerol in 50 mM Tris-HCl pH 9.5. After *in vitro* reactivation, *r*-TOP was concentrated and purified on a Toyopearl HW-55 column. The concentration of peroxidase was measured by absorbance at 403 nm, using the experimentally determined extinction coefficient value of 108.0 ± 0.5 $mM^{-1}cm^{-1}$ for the protein monomer.[23] The resulting preparation was homogeneous as judged by SDS-PAGE. The activity of purified *r*-TOP toward ABTS was about 4100 U/mg and the RZ value was 3.0.

Chemicals. 1-Ethyl-3-(3-(dimethylamino)propyl) carbodiimide (EDC), *N*-hydroxysulfosuccinimide sodium salt (NHS), hydrogen peroxide, 2,2′-azino-bis(3-ethylbenzothiazoline-6-sulfonic acid) (ABTS), sodium acetate, and hemin chloride were high purity reagents from Sigma-Aldrich and were used as received. Sodium phosphate buffer (SPB) solutions were prepared from dihydrogen sodium phosphate (from Fluka) and water purified with a Millipore Milli-Q system (resistivity 18 MΩ cm).

Enzyme Immobilization. Pyrolytic graphite electrodes were constructed by fitting a rod of highly oriented pyrolytic graphite from Mineral Technologies into a PEEK casing, so that it exposed the edge of the graphite planes with a circular geometric area of 0.07 cm^2. Prior to enzyme immobilization, graphite electrodes were polished with abrasive P2400 sandpaper, then they were rinsed with Millipore water and dried with an argon stream.

Physical adsorption and covalent attachment were assayed for immobilization of *r*-TOP on graphite. To physisorb *r*-TOP, a 17 μL drop of 0.11 mg mL^{-1} *r*-TOP in 0.01 M SPB pH 6 was deposited on the graphite surface, and physisoption was allowed to proceed for 20 h at 4 °C. Covalent immobilization was carried out either with or without previous activation of the electrode surface. For covalent coupling with previous surface activation, which from now on will be denoted as *sequential* covalent immobilization, the electrode was incubated for 2 h at 4 °C in a solution formed by mixing a 4.5 μL drop of 20 mM NHS and a 5.5 μL drop of 40 mM EDC,[24] both solutions being also 0.01 M SPB pH 6. After activation of the oxidized species at the graphite surface, the electrode was thoroughly rinsed with water and dried with an argon stream. Then, in a second incubation step that lasted 20 h at 4 °C, the electrode was capped with a 17 μL drop of a 0.11 mg mL^{-1} *r*-TOP solution in 0.01 M SPB pH 6. Covalent coupling without previous surface activation, that from now on will be denoted as *simultaneous* covalent immobilization, was carried out by exposing the electrode surface to a mixture of three droplets: a 4.5 μL drop of 20 mM NHS, a 5.5 μL drop of 40 mM EDC, and a 7 μL drop of a 0.26 mg mL^{-1} *r*-TOP solution that was also 0.01 M SPB pH 6, for 20 h at 4 °C. Irrespective of the immobilization protocol, the enzyme concentration in the deposition solution was 3 μM, and the electrodes were thoroughly rinsed with water and washed with the working buffer solution after enzyme incubation.

Effect of Coupling Reagents on *r*-TOP Aggregation and Activity in Solution. To evaluate the impact of incubation with EDC and NHS on *r*-TOP aggregation, the enzyme was incubated in the same solution as for immobilization on graphite (see above). After 20 h incubation at 4 °C, *r*-TOP was desalted on a Sephadex G-25 column equilibrated with 0.01 M SPB pH 6. Oligomerization was tested by SDS-PAGE. The acrylamide concentration of the resolving gel was 10%. Proteins were stained with SYPRO Ruby protein gel stain. Catalytic activity toward ABTS was measured after incubation according to the method described below and normalized to the Soret absorbance. The reaction mixture contained ABTS (0.36 mM) and H_2O_2 (5 mM) in 100 mM sodium acetate buffer (pH 4.5). The reaction rate was monitored at 405 nm on a UV-2401 (Shimadzu, Japan) spectrophotometer, with a molar absorption coefficient for the ABTS oxidation product taken equal to 36.8 $mM^{-1}cm^{-1}$.[25] One unit of enzymatic activity was defined as the quantity of enzyme necessary to produce 1 μmol of product per minute under the assay conditions. The assays were run at least in triplicate.

Electrochemical Measurements. Linear scan voltammetric measurements were performed with an AUTOLAB PGSTAT 30, from Eco Chemie B.V., in a conventional three electrode undivided glass cell, equipped with a gas inlet and thermostated with a water jacket. The counter and reference electrodes were a Pt bar and a Ag|AgCl/NaCl saturated electrode, respectively. The reference electrode was connected to the cell solution via a salt bridge and kept at room temperature (23 ± 2 °C) in a nonisothermal configuration. Reported potential values have been corrected to the SHE potential scale by adding +192 mV to the experimental potential values. All measurements were carried out under an

DOI: 10.1021/acs.analchem.5b01710
Anal. Chem. XXXX, XXX, XXX−XXX

argon atmosphere. Working solutions contained 20 mM sodium phosphate buffer at the desired pH. Positive feedback for ohmic drop compensation was applied for voltammograms recorded at scan rates higher than 1 V s^{-1}.

RESULTS AND DISCUSSION

Nonturnover Voltammetry of Immobilized *r*-TOP. First, we evaluated the influence of the immobilization protocol on the voltammetric response of immobilized *r*-TOP/graphite electrodes in the absence of hydrogen peroxide. Figure 1A illustrates some typical cyclic voltammograms obtained for *r*-TOP physisorbed on graphite electrodes, where two voltammetric waves associated with the heme Fe(III)/Fe(II) redox couple[26] can be observed and are denoted as peaks I and II, displaying midpoint potentials of −80 mV and +260 mV vs NHE, respectively. Comparison of these midpoint potentials with those obtained with other immobilization protocols (see Table 1), and with formal potentials reported for a variety of heme proteins,[26] shows that peak II appears to be too positive and is likely to be related to denatured *r*-TOP molecules. The two waves merge to some extent and have full widths at half-maximum larger than 100 mV, indicating a distribution of tunneling distances and/or of environments around the electroactive heme groups. It may also be observed that the more anodic wave overlaps with a smaller voltammetric feature which is seen in the absence of enzyme, and it has been attributed[27−29] to the redox conversion of quinone groups present at the graphite electrode surface (see the Supporting Information). The small split between the cathodic and anodic peak potentials observed for each wave at high scan rates is indicative of a surprisingly fast electron exchange rate. In fact, standard electron transfer rate constants close to 300 s^{-1} can be estimated from the scan rate dependence of the separation of the peak potentials according to Laviron's approach[30] (see the Supporting Information). The surface concentration of electrochemically active heme groups was determined by integration of the area under the baseline corrected voltammetric peaks between −0.35 and 0.55 V (see Q/FA values in Table 1) and subtraction of the charge due to the graphite quinone groups (0.17 ± 0.02 μC), and it was found to be Γ_{heme} = 79 ± 15 pmol cm^{-2}.

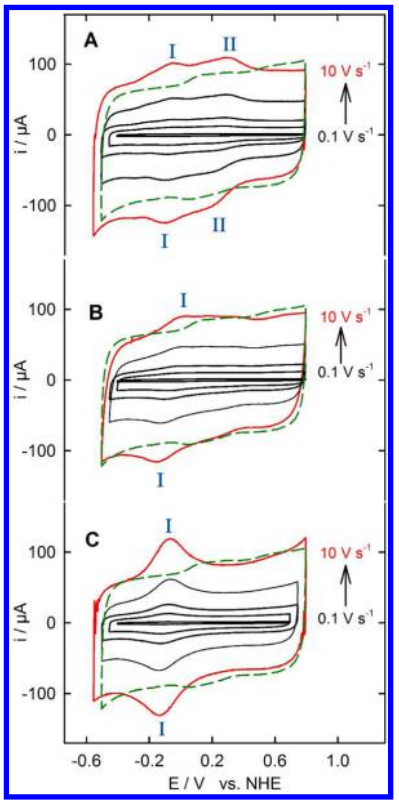

Figure 1. Scan rate dependence of nonturnover cyclic voltammograms recorded in the presence of 0.02 M SPB pH 7 at 0 °C, corresponding to each of the three protocols of *r*-TOP immobilization. (A) physisorption, (B) *sequential* covalent immobilization and (C) *simultaneous* covalent immobilization. Scan rates in V s^{-1}: 0.1, 1, 2, 5, and 10 (red line). The green broken line is a background voltammogram recorded at 10 V s^{-1} under the same experimental conditions but in the absence of *r*-TOP. Blue labels I and II help to identify voltammetric peaks associated with *r*-TOP redox conversion.

A voltammetric response consisting of a well-developed peak (peak I) and an anodic shoulder is observed when *r*-TOP is bound to the graphite surface via the *sequential* immobilization protocol (Figure 1B). Peak I displays a midpoint potential of −72 mV for the Fe(III)/Fe(II) redox couple, a value close to that obtained for the more cathodic peak with the physisorption protocol. The split between the cathodic and anodic peak potentials remains low upon increasing the scan rate (ΔE_p= 195 mV at 100 V s^{-1}) and is again consistent with a high value of the electron transfer rate constant (k_S = 280 s^{-1}). Integration of the baseline-corrected voltammetric current and subtraction of the charge associated with the graphite quinone groups provides a surface concentration of electroactive heme groups Γ_{heme} = 45 ± 8 pmol cm^{-2}, approximately half the number obtained from physisorbed *r*-TOP, which suggests that a significant portion of the immobilized enzymes have adopted

Table 1. Electrochemical Characteristics of the Nonturnover Fe(III)/Fe(II) Redox Conversion of Immobilized *r*-TOP and Hemin

immobilization protocol	$E_{1/2}$[a] vs NHE (mV)	Q/FA[b] (pmol cm^{-2})	Γ_{heme}[d] (pmol cm^{-2})	k_S[c] (s^{-1})
physisorption	−80 ± 8[e]	104 ± 15	79 ± 15	300 ± 30[e]
	260 ± 10[f]			280 ± 30[f]
sequential chemisorption	−72 ± 12[e]	70 ± 8	45 ± 8	280 ± 30[e]
simultaneous chemisorption	−100 ± 10[e]	111 ± 17	86 ± 17	350 ± 30[e]
hemin physisorbed	−130 ± 12	580 ± 15	555 ± 15	20 ± 2

[a]Estimated as the average peak potential. [b]Determined by integration of the voltammetric peaks from −0.35 V to 0.55 V. [c]Estimated from peak separation by Laviron's method. [d]Determined by integration of the voltammetric peaks and subtraction of quinone background charge (25 ± 2 pmol cm^{-2}). [e]Values corresponding to Peak I in Figure 1. [f]Values corresponding to Peak II in Figure 1.

DOI: 10.1021/acs.analchem.5b01710
Anal. Chem. XXXX, XXX, XXX−XXX

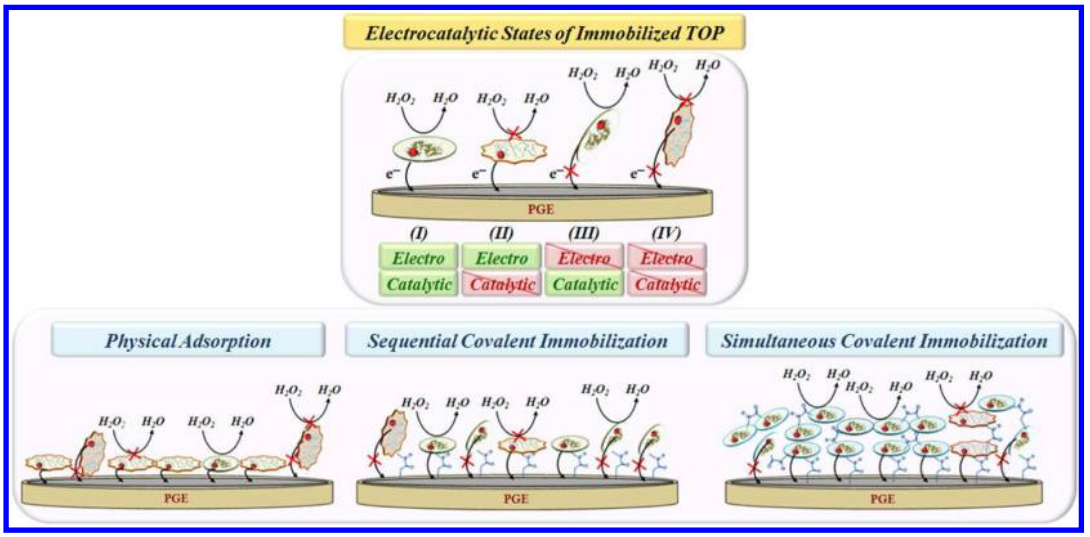

Figure 2. (Upper panel) Schematic representation of the four states that are considered relevant to discuss the electrocatalytic properties of immobilized *r*-TOP molecules. Electron transfer (black arrows) is assumed to take place between the heme group (red circle) of properly oriented enzymes and graphite (gray surface). Catalytic function is allowed for proteins that retain their native structure (smooth ellipses), but forbidden for denatured proteins (starred ellipses). (Lower panels) Schematic representation of the modified electrode after *r*-TOP immobilization on the graphite surface according to the indicated protocol. New amide bonds formed during enzyme immobilization are highlighted in blue.

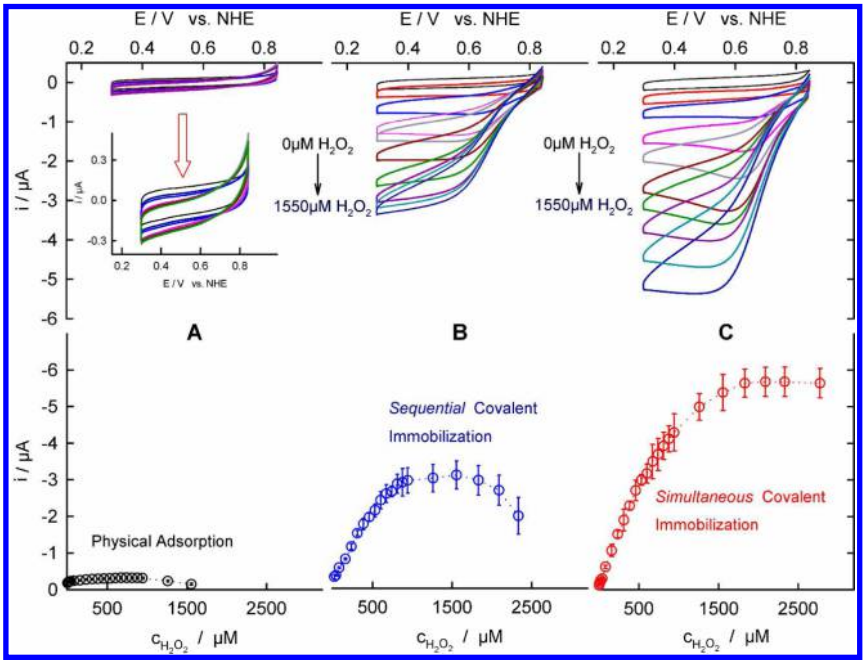

Figure 3. Cyclic voltammograms recorded at 0.01 V s^{-1} (top panels) and voltammetric currents at 0.3 V (bottom panels) for *r*-TOP modified graphite electrodes after successive additions of hydrogen peroxide to the cell solution. Protocol of *r*-TOP immobilization: (A) physisorption, (B) *sequential* covalent attachment, and (C) *simultaneous* covalent attachment. Other experimental conditions, 0.02 M SPB pH 7 and 0 °C.

inadequate orientations for electron exchange with the electrode.

On the other hand, the *simultaneous* immobilization protocol produces remarkably well-defined voltammetric waves (Figure 1C) that display a midpoint potential of −100 mV and are somewhat wider (fwhm = 213 mV) than those obtained with the two previous protocols. The voltammetric features associated with surface quinone groups are no longer visible, but their presence is still evident when the Fe(III)/Fe(II) currents are lowered by decreasing the protein deposition time. As before, high scan rates are required to increase the peak separation (ΔE_p = 135 mV at 100 V s^{-1}), and Laviron's analysis of the trumpet plot gives a value of k_S = 350 s^{-1}. This *simultaneous* protocol results in a number of electroactive heme groups Γ_{heme} = 86 ± 17 pmol cm^{-2} similar to that found with the physisorption protocol (compare the three red voltammograms in Figure 1).

Since the surface concentration of a compact *r*-TOP monolayer is estimated to be 31 pmol cm^{-2},[31] it would appear at first sight that these voltammetric experiments are sampling a multilayered enzymatic structure. However, it should be pointed out that the microscopic surface area of edge-plane graphite electrodes accessible for protein adsorption is not known. Blanford and Armstrong[32] used nitrogen porosimetry

DOI: 10.1021/acs.analchem.5b01710
Anal. Chem. XXXX, XXX, XXX−XXX

Table 2. Comparison of the Analytical Performance of *r*-TOP/Graphite and HRP-Based Hydrogen Peroxide Biosensors

electrode[a]	detection limit (μM)	sensitivity (A M^{-1} cm^{-2})	linear range (μM)	$E_{calibration}$ (V vs NHE)	ref
TOP *sequential* chemisorption	3 (0.08)	0.055 (0.09)[b]	10−700	0.3	this work
TOP *simultaneous* chemisorption	2 (0.09)	0.080 (0.05)[b]	10−900	0.3	this work
HRP clay-chitosan-AuNP/GCE	9	0.009	39−3100	−0.1	35
HRP cross-linked AuNP/Au	1.5	0.5×10^{-3}	5−1100	0.2	36
HRP Ag@CNC/ITO	0.02		0.5−140	−0.1	37
HRP SWCNT/SPCE	0.4	5.1×10^{-3}	0.5−500	0.1	38
HRP RTIL-AuNP-TNT-Nafion/GCE	2.1	0.012	5−1000	−0.2	39

[a]AuNP: gold nanoparticles; GCE: glassy carbon electrode; Ag@CNC: nanocomposite with Ag core and carbon coating; ITO: indium−tin oxide electrode; SWCNT: single-wall carbon nanotubes; SPCE: screen-printed carbon electrode; RTIL: room temperature ionic liquid; TNT: titanate nanotubes. [b]Relative standard deviations are given in parentheses.

and scanning electron microscopy to characterize the surface of these electrodes, after they were subjected to a polishing procedure. They obtained a BET surface area $\sim 10^4$ times greater than the geometric surface area and concluded that the maximum coverage for protein adsorption was likely to lie within the 100−1000 pmol cm^{-2} range for an electrode surface that is assumed to be planar. Therefore, these electrodes seem to provide enough surface area to accommodate the number of proteins required to produce the Γ_{heme} values listed in Table 1 and, moreover, it should be noted that only heme groups that are close to the electrode surface are likely to be involved in such a fast electron exchange with the electrode (see Figure 2). In a separate experiment, free heme groups from hemin chloride were physisorbed under similar experimental conditions, giving rise to an electroactive surface concentration of 580 pmol cm^{-2}. The voltammetric response of these free heme groups was characterized by a midpoint potential of −130 mV, i.e., somewhat more negative than the $E_{1/2}$ values obtained for *r*-TOP, and a standard electron transfer rate constant of 20 s^{-1}, i.e., much lower than the values we have recorded for *r*-TOP, in reasonable agreement with previous reports in the literature.[33] Therefore, the most likely physical scenario is one in which the nonturnover voltammetric peaks in Figure 1 are generated by a mixed population of heme groups that are close to the electrode surface and remain coordinated to some amino acid residues to facilitate a fast electron transfer. Some of these heme groups would be coordinated to peptide residues from denatured proteins, while others would retain its original location within the intact protein structure and would be responsible for the bioelectrocatalytic response that will be described in the next section. Out of the three immobilization procedures considered, only the voltammetric response associated with the *simultaneous* immobilization protocol combines a large faradaic charge at high scan rates, which suggests a proper orientation and/or a preserved quaternary structure of most immobilized proteins (as opposed to the case of the *sequential* immobilization protocol), with a relatively narrow potential range for electron transfer, indicative of a moderate degree of denaturation (as opposed to the case of the physisorption protocol).

Bioelectrocatalysis of Immobilized *r*-TOP. The fast electron transfer kinetics observed between the heme groups of *r*-TOP and graphite under nonturnover conditions satisfy a first requirement to use this enzyme as a building block of a H_2O_2 biosensor. A second requirement is that the enzyme retains its catalytic activity upon immobilization on the electrode. In this regard, the immobilization procedure is likely to play a key role in order to orient properly the protein and minimize the denaturing influence of the electrode surface on the protein structure.

Figure 3 illustrates the influence of hydrogen peroxide concentration on the voltammetric response of immobilized *r*-TOP between 0.3 and 0.85 V vs SHE, a potential window where the catalytic reduction of H_2O_2 takes place via the reduction of Compound I and Compound II intermediates.[6] As can be seen, significant differences are observed in Figure 3 between the electrocatalytic responses generated by the three immobilization protocols.

Physically adsorbed *r*-TOP develops rather low catalytic waves (top panel in Figure 3A), whose flattened shape is analogous to that previously reported for *r*-TOP physisorbed on either graphite[11] or gold[10] electrodes. Moreover, this catalytic signal becomes quickly saturated even in the presence of low (~0.1 mM) hydrogen peroxide concentrations, thereby restricting the linear range of response of the biosensor. Since a significant population of heme groups displays fast electron transfer kinetics under the same immobilization conditions (see above), it is likely that these electrocatalytic limitations reflect an extensive denaturation of the enzymes upon physisorption at the graphite surface.

On the other hand, covalent attachment of *r*-TOP to the graphite surface, by either the *sequential* or the *simultaneous* immobilization protocol, produces well-developed electrocatalytic waves (upper panels in Figure 3B,C) and calibration plots with a wide linear range (lower panels in Figure 3). However, there are some clear differences between the electrochemical responses generated by these two protocols. While the *sequential* protocol gives rise to S-shaped voltammograms, characteristic of enzymatic kinetic control,[34] the *simultaneous* immobilization protocol produces steeper and peak-shaped voltammograms, characteristic of substrate diffusion control, as it would be expected for a larger surface concentration of catalytically active enzymes involved in direct electron transfer with the electrode. It is interesting to note that the analytical parameters obtained from the *simultaneous* protocol, as derived directly from these low scan rate voltammograms without accounting for H_2O_2 mass transfer effects, take values (see Table 2) similar to those recently reported for more complex biosensors based on immobilized HRP.[35−39] Within this context, the experimental simplicity of the *simultaneous* protocol should also be stressed, since it makes use of easily available reagents in a single preparative step, while most of the electrodes listed in Table 2 (except for the case of the SWCNT/SPCE electrode) require a sequence of preparative steps, including often the synthesis of key components.

DOI: 10.1021/acs.analchem.5b01710
Anal. Chem. XXXX, XXX, XXX−XXX

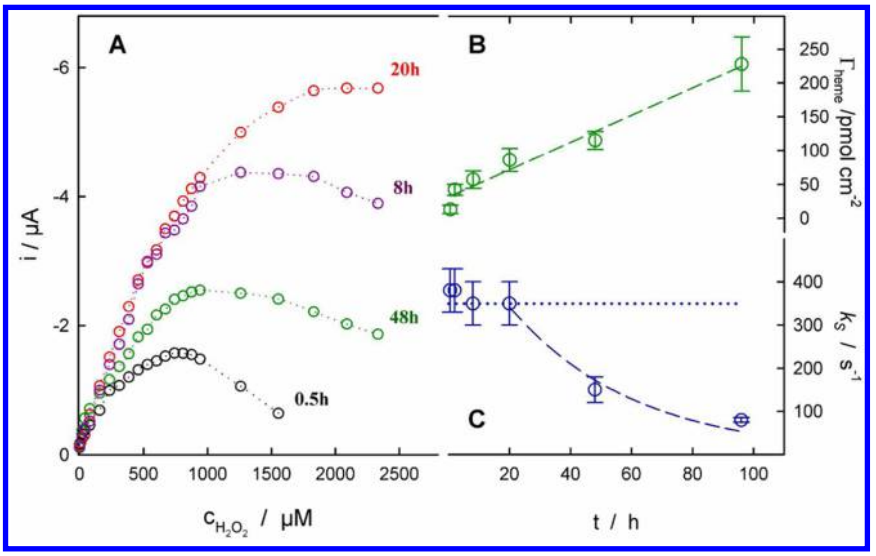

Figure 4. Influence of the indicated incubation time for *simultaneous* immobilization of *r*-TOP at graphite electrodes on (A) voltammetric currents recorded at 0.3 V with v = 0.01 V s^{-1}, (B) surface concentration of electroactive heme groups, and (C) their standard electron transfer rate constant. Broken and dotted lines are just guides for the eye. Other experimental conditions: 0.02 M SPB pH 7 and 0 °C.

As can be observed in the lower panels of Figure 3, catalytic currents start to decrease when the H_2O_2 concentration exceeds a critical value, which is larger for the *simultaneous* (~2.5 mM) than for the *sequential* (~1.5 mM) immobilization protocol and decreases upon increasing the working temperature (see the Supporting Information). This behavior is due to the inhibitory effect that H_2O_2 exerts on peroxidases through two main kinetic routes, the first leading to the slow and irreversible formation of a verdohemoprotein while the second involves the reversible formation of Compound III.[40] A similar increase in the critical concentration of H_2O_2 was observed when the mediated electrochemical response of graphite electrodes modified with one and four monolayers of biotinylated HRP were compared.[41] This effect was explained quantitatively as a direct consequence of the increased number of active enzymes that were present in the multilayered enzymatic structure. Given the kinetic and structural similarities between TOP and HRP isoenzyme A,[7,42] the same reasoning should apply in our case, implying that the *simultaneous* immobilization protocol produces a larger number of electrocatalytically active enzymes than the *sequential* protocol, thereby confirming the preliminary conclusion we reached by comparing their voltammetric shapes.

To address the question of *r*-TOP oligomerization in the course of the *simultaneous* immobilization protocol, we analyzed with SDS-PAGE the protein molecular weight distribution after incubating *r*-TOP under the same conditions and obtained exclusively the dimeric form (see Figure S5). Moreover, 20 h incubation of *r*-TOP with the cross-linking reagents results in a 15% loss of catalytic activity only (from 4100 to 3500 U/mg). This preservation of the catalytic activity in solution after *r*-TOP cross-linking should be considered as the result of both dimerization and intramolecular fixation of the *r*-TOP surface, making the molecule more conformationally stable against prolonged incubation and interaction with the electrode surface. We have also checked the electrocatalytic activity of these *r*-TOP dimers under conditions that mimic those of the *sequential* and *simultaneous* protocols. First we incubated *r*-TOP and the coupling reagents for 18 h, as described previously, to form the dimers in solution, and then we put into contact for 2 h the incubated solution with either the bare graphite surface, as in the *simultaneous* protocol, or a graphite surface modified with the coupling reagents, as in the *sequential* protocol. In both cases, electrocalytic currents are higher than those obtained with the *sequential* protocol and, when dimers were immobilized on the bare graphite surface, electrocatalytic currents become quite close to those recorded with the *simultaneous* protocol (see Figure S6). The improvement of the catalytic response, when the sequential protocol is applied to *r*-TOP dimers rather than to *r*-TOP monomers, suggests that the concomitant formation of inter- and intramolecular amide bonds deactivates a significant portion of the amine groups that anchor the enzyme to the electrode with inefficient orientations for electron transfer. Out of nine possible anchoring centers (i.e., the eight lysines and the N-terminus located in Gln1) most lysines are either buried into the polypeptide matrix or oriented toward a neighbor carboxy group, so that intramolecular amide bond formation is favored over its intermolecular counterpart. Lys111 and the N-terminus are the two amine residues most exposed to the external solution and, therefore, the most probable candidates for amide bonding with the electrode surface after incubation with the coupling reagents. Out of these two possibilities, which are illustrated in Figure S7, attachment through Lys111 is expected to produce a more favorable orientation for electron exchange with the electrode. On the other hand, the remarkable similarity between the catalytic currents obtained when either *r*-TOP monomers or dimers are subjected to the *simultaneous* protocol (see Figure S7) suggests that inter- and intramolecular amide bonds form faster than graphite-protein amide bonds. It should be noted that only the first layer of enzymes contacting the electrode surface can be involved in direct electron transfer and that their covalent interaction with the electrode is essentially the same in the *sequential* and *simultaneous* protocols (Figure 2). Thus, it seems likely that the higher catalytic activity observed with the last protocol should be related to a higher percentage of adsorbed proteins that have an appropriate orientation with respect to the electrode surface and preserve their native structure upon immobilization. It has been shown recently that *r*-HRP monomers and dimers "hydrophobized"

DOI: 10.1021/acs.analchem.5b01710
Anal. Chem. XXXX, XXX, XXX−XXX

after treatment with glutaraldehyde display an improved stability upon adsorption on graphite electrodes.[21] In a similar way, intramolecular amide bonds developed in the *simultaneous* protocol can help to preserve the native structure of immobilized *r*-TOP molecules.

Amide bonds within and between TOP molecules in solution and between TOP molecules and the graphite surface are continuously being formed during the incubation step in the *simultaneous* immobilization protocol. Therefore, the degree of interprotein bonding of the first enzymatic layer and its catalytic properties are expected to evolve with the incubation time. In fact, Figure 4A shows how the linear response range increases with the incubation time until it reaches its largest value for 20 h of incubation. However, larger incubation times become detrimental for the biosensor performance, revealing the presence of two conflicting effects of the incubation process on the activity of the enzymatic film.

Upon increasing the incubation time, we observe a continuous increase in the number of electroactive heme groups (Figure 4B), some of which presumably belong to denatured proteins. However, the electron transfer rate constant values do not display a monotonous variation with the incubation time (Figure 4C). They remain nearly constant and close to 350 s^{-1} up to ~20 h, and then they decrease down to 90 s^{-1} for a ~ 96 h incubation. This behavior points to the onset of structural changes in the catalytic film for incubation times exceeding 20 h. Therefore, it seems reasonable to conclude that the number of active enzymes in the catalytic layer increases during the first 20 h of incubation and that this initial increase in the number of enzymes does not alter the interprotein interactions that produce a convenient protein orientation and protect the enzymatic function against H_2O_2-induced deactivation, as it has been shown in the case of HRP polymers in solution.[19,20] This favorable situation results in an improvement of both the linear response range and the long-term stability of the biosensor with the incubation time (see the Supporting Information). However, a further increase in the accumulation of extensively cross-linked proteins seems to cause conformational changes in those enzyme molecules that are involved in direct electron exchange with the electrode, resulting in their progressive denaturation, loss of catalytic activity and resistance against H_2O_2-induced deactivation.

CONCLUSIONS

Surface immobilized *r*-TOP displays a very fast electron exchange with graphite electrodes, which makes this enzyme a good candidate for developing third generation H_2O_2 biosensors. Covalent attachment to the electrode surface, employing the usual two-step carbodiimide coupling process, produces a significant improvement of the electrocatalytic response with respect to that obtained from physisorbed enzymes. However, its linear response range and stability is limited by H_2O_2-induced inhibition. In this work we have shown that these problems can be alleviated by using a simpler one-step protocol, where enzyme and electrode are simultaneously incubated with the cross-coupling reagents 1-ethyl-3-(3-(dimethylamino)propyl) carbodiimide and *N*-hydroxysulfosuccinimide during the deposition process. An optimized incubation time of 20 h has been found to produce a biosensor that can operate up to a 2 mM H_2O_2 concentration at 0 °C and that retains 65% of its initial activity after 20 days of operation. The remarkably improved electrocatalytic properties of this biosensor can be attributed to an efficient electronic coupling between tobacco peroxidase and graphite and to the formation of intra- and intermolecular amide bonds that stabilize the protein structure and reduce the percentage of anchoring groups that provide an inadequate orientation for electron exchange with the electrode.

ASSOCIATED CONTENT

Supporting Information

The Supporting Information is available free of charge on the ACS Publications website at DOI: 10.1021/acs.analchem.5b01710.

Comparison of the voltammetric responses, trumpet plots for the determination of the electron transfer standard rate constant of the Fe(III)/Fe(II) redox couple, long-term stability of the electrocatalytic current, effect of temperature on the electrocatalytic response of *r*-TOP, SDS-PAGE of *r*-TOP before and after incubation with coupling reagents, electrocatalytic activity of preincubated dimers, and molecular location of likely binding sites for *r*-TOP after reaction with coupling reagents (PDF)

AUTHOR INFORMATION

Corresponding Author

*E-mail: fondacab@us.es. Phone: (0034)-955421002.

Notes

The authors declare no competing financial interest.

ACKNOWLEDGMENTS

J. L. O., J. J. C., and R. A. acknowledge financial support from the Spanish Ministry of Economy and Competitiveness (Grants CTQ2008-00371 and CTQ2014-52641-P) and L.G. from the Swedish Research Council (Grant 2014-5908). The authors thank Dr. I. G. Gazaryan for valuable comments on the manuscript.

REFERENCES

(1) Cracknell, J. A.; Vincent, K. A.; Armstrong, F. A. *Chem. Rev.* **2008**, *108*, 2439−2461.

(2) Chen, W.; Cai, S.; Ren, Q.; Wen, W.; Zhao, Y. *Analyst* **2012**, *137*, 49−58.

(3) Meredith, M. T.; Minteer, S. D. *Annu. Rev. Anal. Chem.* **2012**, *5*, 157−79.

(4) Lopes, G. R.; Pinto, D. C. G. A.; Silva, A. M. S. *RSC Adv.* **2014**, *4*, 37244−37265.

(5) Ruzgas, T.; Lindgren, A.; Gorton, L.; Hecht, H. J.; Reichelt, J.; Bilitewski, U. In *Electroanalytical Methods for Biological Materials*; Chambers, J. Q., Brajter-Toth, A., Eds.; Marcel Dekker: New York, 2002; pp 233−275.

(6) Ferapontova, E. E. *Electroanalysis* **2004**, *16*, 1101−1112.

(7) Gazaryan, I. G.; Lagrimini, L. M. *Phytochemistry* **1996**, *41*, 1029−1034.

(8) Gazaryan, I. G.; Ouporov, I. V.; Chubar, T. A.; Fechina, V. A.; Mareeva, E. A.; Lagrimini, L. M. *Biochemistry (Moscow)* **1998**, *63*, 600−606.

(9) Gazaryan, I. G.; Gorton, L.; Ruzgas, T.; Csöregi, E.; Schuhmann, W.; Lagrimini, L. M.; Khushpulian, D. M.; Tishkov, V. I. *J. Anal. Chem.* **2005**, *60*, 558−566.

(10) Ferapontova, E. E.; Castillo, J.; Hushpulian, D.; Tishkov, V.; Chubar, T.; Gazaryan, I.; Gorton, L. *Electrochem. Commun.* **2005**, *7*, 1291−1297.

(11) Castillo, J.; Ferapontova, E. E.; Hushpulian, D.; Tasca, F.; Tishkov, V.; Chubar, T.; Gazaryan, I.; Gorton, L. *J. Electroanal. Chem.* **2006**, *588*, 112−121.

DOI: 10.1021/acs.analchem.5b01710
Anal. Chem. XXXX, XXX, XXX−XXX

(12) Munteanu, F. D.; Lindgren, A.; Emnéus, J.; Gorton, L.; Ruzgas, T.; Csöregi, E.; Ciucu, A.; Van Huystee, R. B.; Gazaryan, I. G.; Lagrimini, L. M. *Anal. Chem.* **1998**, *70*, 2596−2600.
(13) Munteanu, F. D.; Gorton, L.; Lindgren, A.; Ruzgas, T.; Emnéus, J.; Csöregi, E.; Gazaryan, I. G.; Ouporov, I. V.; Mareeva, E. A.; Lagrimini, L. M. *Appl. Biochem. Biotechnol.* **2000**, *88*, 321−333.
(14) Lindgren, A.; Ruzgas, T.; Gorton, L.; Csöregi, E.; Ardila, G. B.; Sakharov, I. Y.; Gazaryan, I. G. *Biosens. Bioelectron.* **2000**, *15*, 491−497.
(15) Gaspar, S.; Popescu, I. C.; Gazaryan, I. G.; Bautista, A. G.; Sakharov, I. Y.; Mattiasson, B.; Csöregi, E. *Electrochim. Acta* **2000**, *46*, 255−264.
(16) Gaspar, S.; Zimmermann, H.; Gazaryan, I. G.; Csöregi, E.; Schuhmann, W. *Electroanalysis* **2001**, *13*, 284−288.
(17) Ortega, F.; Domínguez, E.; Burestedt, E.; Emnéus, J.; Gorton, L.; Marko-Varga, G. *J. Chromatogr. A* **1994**, *675*, 65−78.
(18) Shleev, S.; Tkac, J.; Christenson, A.; Ruzgas, T.; Yaropolov, A. I.; Whittaker, J. W.; Gorton, L. *Biosens. Bioelectron.* **2005**, *20*, 2517−2554.
(19) Hoshino, N.; Nakajima, R.; Yamazaki, I. *J. Biochem.* **1987**, *102*, 785−791.
(20) Budnikova, L. P.; Eryomin, A. N. *Appl. Biochem. Microbiol.* **2006**, *42*, 127−133.
(21) Ignatenko, O. V.; Sjölander, A.; Hushpulian, D. M.; Kazakov, S. V.; Ouporov, I. V.; Chubar, T. A.; Poloznikov, A. A.; Ruzgas, T.; Tishkov, V. I.; Gorton, L.; Klyachko, N. L.; Gazaryan, I. G. *Adv. Biosens. Bioelectron.* **2013**, *2*, 25−34.
(22) Hushpulian, D. M.; Savitski, P. A.; Rojkova, A. M.; Chubar, T. A.; Fechina, V. A.; Sakharov, I. Y.; Lagrimini, L. M.; Tishkov, V. I.; Gazaryan, I. G. *Biochemistry (Moscow)* **2003**, *68*, 1189−1194.
(23) Gazaryan, I. G.; Lagrimini, L. M.; George, S. J.; Thorneley, R. N. *Biochem. J.* **1996**, *320*, 369−372.
(24) Vaz-Dominguez, C.; Campuzano, S.; Rüdiger, O.; Pita, M.; Gorbacheva, M.; Shleev, S.; Fernandez, V. M.; De Lacey, A. L. *Biosens. Bioelectron.* **2008**, *24*, 531−537.
(25) Smith, A.; Santama, N.; Dacey, S. *J. Biol. Chem.* **1990**, *265*, 13335−13343.
(26) Battistuzzi, G.; Bellei, M.; Bortolotti, C. A.; Sola, M. *Arch. Biochem. Biophys.* **2010**, *500*, 21−36.
(27) Evans, J. F.; Kuwana, T.; Henne, M. T.; Royer, G. P. *J. Electroanal. Chem. Interfacial Electrochem.* **1977**, *80*, 409−416.
(28) Csöregi, E.; Jönsson-Petterson, G.; Gorton, L. *J. Biotechnol.* **1993**, *30*, 315−337.
(29) Lu, M.; Compton, R. G. *Analyst* **2014**, *139*, 2397−2403.
(30) Laviron, E. *J. Electroanal. Chem. Interfacial Electrochem.* **1979**, *101*, 19−28.
(31) Ferapontova, E. E.; Grigorenko, V. G.; Egorov, A. M.; Börchers, T.; Ruzgas, T.; Gorton, L. *Biosens. Bioelectron.* **2001**, *16*, 147−157.
(32) Blanford, C. F.; Armstrong, F. A. *J. Solid State Electrochem.* **2006**, *10*, 826−832.
(33) Chen, J.; Wollenberger, U.; Lisdat, F.; Ge, B.; Scheller, F. W. *Sens. Actuators, B* **2000**, *70*, 115−120.
(34) Limoges, B.; Savéant, J. M.; Yazidi, D. *J. Am. Chem. Soc.* **2003**, *125*, 9192−9203.
(35) Zhao, W.; Mai, Z.; Kang, X.; Zou, X. *Biosens. Bioelectron.* **2008**, *23*, 1032−1038.
(36) Villalonga, R.; Díez, P.; Yáñez-Sedeño, P.; Pingarrón, J. M. *Electrochim. Acta* **2011**, *56*, 4672−4677.
(37) Mao, S.; Long, Y.; Li, W.; Tu, Y.; Deng, A. *Biosens. Bioelectron.* **2013**, *48*, 258−262.
(38) Chekin, F.; Gorton, L.; Tapsobea, I. *Anal. Bioanal. Chem.* **2015**, *407*, 439−446.
(39) Liu, X.; Feng, H.; Rui, Y.; Zhao, R.; Wang, Y.; Liu, X. *Biosens. Bioelectron.* **2012**, *31*, 101−104.
(40) Vlasits, J.; Jakopitsch, C.; Bernroitner, M.; Zamocky, M.; Furtmüller, P. G.; Obinger, C. *Arch. Biochem. Biophys.* **2010**, *500*, 74−81.
(41) Andrieux, C. P.; Limoges, B.; Savéant, J. M.; Yazidi, D. *Langmuir* **2006**, *22*, 10807−10815.
(42) Dunford, H. B. *Heme Peroxidases*; Wiley-VCH: New York, 1999.

DOI: 10.1021/acs.analchem.5b01710
Anal. Chem. XXXX, XXX, XXX−XXX